Neuron, volume 57

Supplemental Data

Ivy Cells: A Population of Nitric-Oxide-Producing, Slow-Spiking GABAergic Neurons and Their Involvement in Hippocampal Network Activity

Pablo Fuentealba, Rahima Begum, Marco Capogna, Shozo Jinno, László F. Márton, Jozsef Csicsvari, Alex Thomson, Peter Somogyi, and Thomas Klausberger

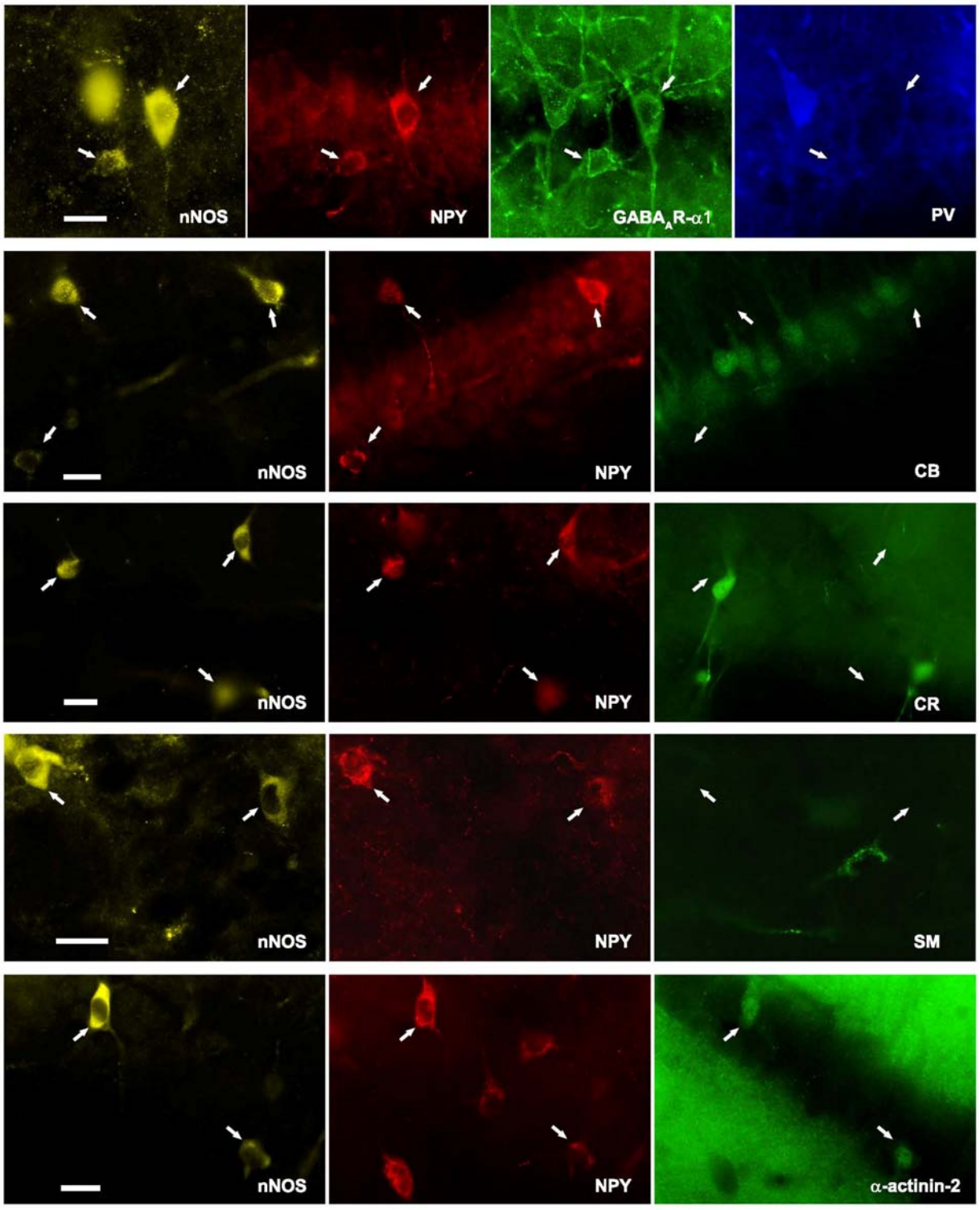

Figure S1. Molecular expression profile of putative Ivy cells. Fluorescent micrographs show putative Ivy cells (arrows) in and around stratum pyramidale identified by the co-localization of nNOS, NPY and in the top panel the α1 subunit of the $GABA_A$ receptor. Putative Ivy cells are immunonegative for the Ca^{2+}-binding proteins PV, CB, CR, or the neuropeptide somatostatin (SM). On the other hand, a large fraction of putative Ivy cells showed somatic labeling for α-actinin-2. Scale bars 20 μm.

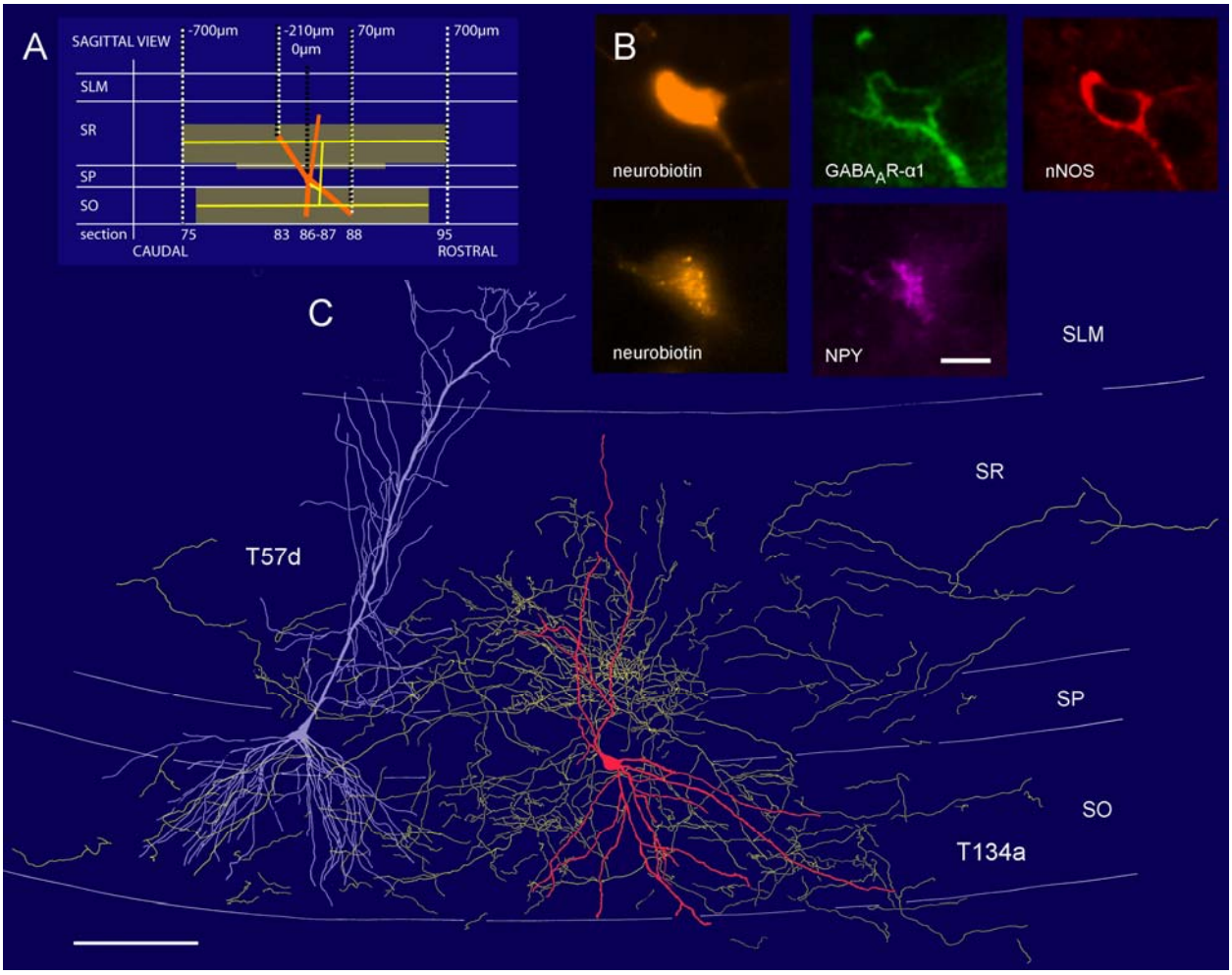

Figure S2. An Ivy cell with a large axonal field spanning three layers recorded *in vivo*. (A) Schematic sagittal view and rostro-caudal extent of the axonal and dendritic arborizations of cell T134a. (B) Fluorescence micrographs of the soma cut in half during sectioning. The recorded cell is immunopositive for nNOS and GABA$_A$R-α1 in one half of the soma, and NPY in the other half. For examples of the firing patterns of this cell, see Supplementary Figure 3. (C) Reconstruction of the soma and dendrites (orange) are shown from three sections, the axon (yellow) is shown only from four 70-µm-thick sections for clarity. Note the very dense axon in both stratum oriens and proximal radiatum. A pyramidal cell (blue, T57d) recorded and labeled in another animal, is added for illustrating spatial relationships. Scale bars: (B) 10 µm; (C) 100 µm.

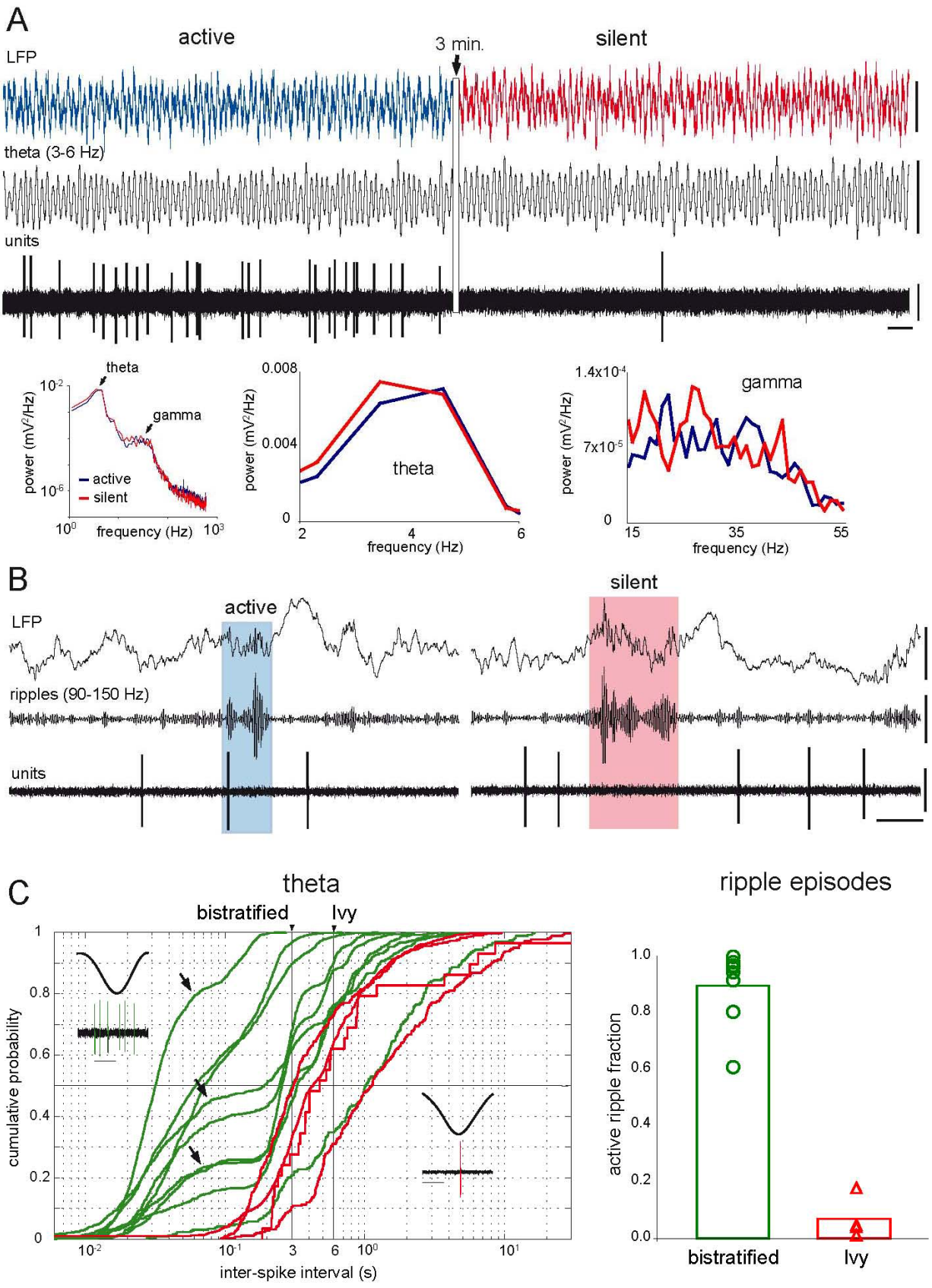

Figure S3. Variability in the firing patterns of Ivy cells during network oscillations and comparison with bistratified cells. (A) Transitions from engagement into firing at almost every

oscillatory cycle to long, silent epochs (> 20 s) could take place within the same period of sustained theta oscillations. Left, examples of the local field potential (LFP, 0.3-300 Hz), LFP filtered for theta oscillations (3-6 Hz) and the single unit activity (units, 0.8-5 kHz) from an identified Ivy cell (T134a). The cell discharges (mean = 1.35 Hz) in some consecutive theta cycles, rarely more than one spike per cycle. Right, from the same theta period as left, but three minutes later; the cell fired at a low rate (0.05 Hz), even though the theta and gamma power, and general power distribution have not changed (bottom panels). (B) Examples of firing activity of another identified Ivy cell (T98e) around ripple oscillations. Note the cell discharging during one of the ripple episodes (left), whereas it remained silent in the next (right). (C) Left, cumulative probability function for the inter-spike intervals from identified Ivy (red) and bistratified (green) cells during theta oscillations. Solid vertical lines indicate average median values. Ivy cells discharged at significantly longer intervals than bistratified cells (0.6 ± 0.2 vs. 0.3 ± 0.1 s, respectively; $P = 0.034$), and also fired at significantly lower frequencies ($P = 0.024$), and also with lower probability ($P = 0.016$) than bistratified cells throughout theta oscillations (0.7 ± 0.4 vs. 5.4 ± 2.4 Hz, and 0.025 ± 0.010 vs. 0.133 ± 0.150, respectively). The mean phase preference of Ivy cells (30.7 ± 63.1°) was significantly different ($P = 0.02$, two-sample exact permutation test) from that of bistratified cells (1 ± 60°). Bumps in the interspike interval distributions of most bistratified cells (arrows) result from high frequency activity (> 10 Hz) during individual theta cycles, which do not occur for Ivy cells. Insets, bistratified cells usually fire multiple action potentials during one theta cycle (green spikes), but Ivy cells rarely discharge more than one spike (red). Right, fraction of ripple episodes, during which Ivy (red) and bistratified (green) cells were active (discharged at least one action potential). Both discharge frequency and probability were significantly lower in Ivy than in bistratified cells ($P = 0.006$ and $P = 0.004$, respectively) during ripple oscillations. Symbols represent individual cells and rectangles indicate averages. Vertical scale bars (A) LFP, theta, and units 0.5 mV; (B) LFP 1 mV, ripples 0.2 mV, units 0.5 mV. Horizontal scale bars (A) 1 s; (B) 200 ms; (C) 100 ms.

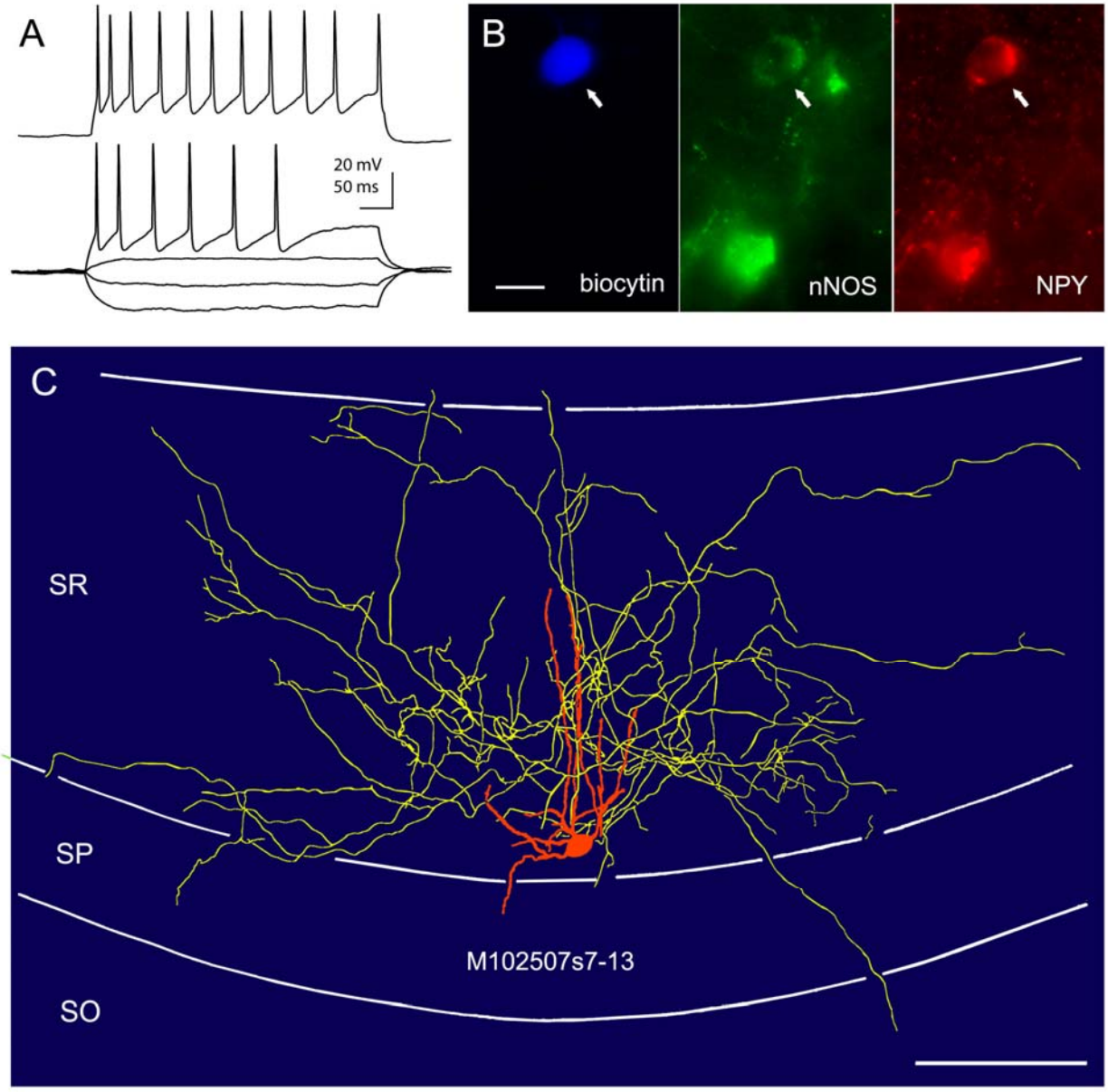

Figure S4. Axonal and dendritic distribution, molecular expression profile and *in vitro* spike trains of an Ivy cell recorded and labeled in stratum radiatum. (A) Voltage responses elicited by current pulses (-60, -20, +20, +80, +120 pA) injected to an Ivy cell (M102507s7-13). (B) Immunofluorescence micrographs of the recorded Ivy cell demonstrating that the cell was immunopositive for nNOS and NPY (soma, left). Note a second nNOS/NPY immunopositive neuron (bottom) that was not recored. (C) Reconstruction of the soma, dendrites (red) and axonal processes (yellow) of the recorded Ivy cell from two 70 μm thick sections. SR, stratum radiatum; SP, stratum pyramidale; SO, stratum oriens. Scale bars: (B),10 μm; (C), 100 μm.

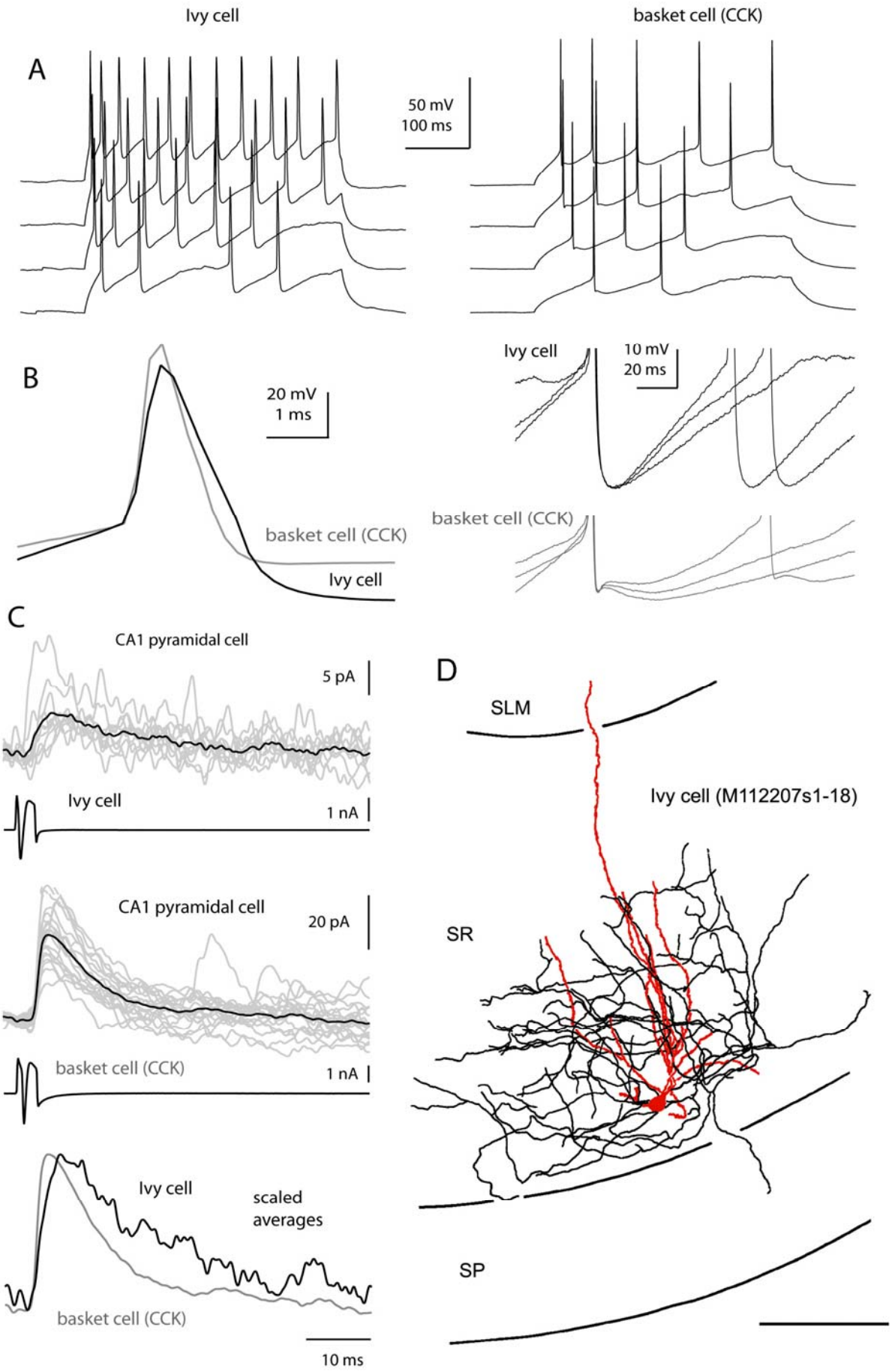
Ivy cell
basket cell (CCK)
A
50 mV
100 ms
B
20 mV
1 ms
basket cell (CCK)
Ivy cell
Ivy cell
10 mV
20 ms
basket cell (CCK)
C
CA1 pyramidal cell
5 pA
Ivy cell
1 nA
CA1 pyramidal cell
20 pA
basket cell (CCK)
1 nA
Ivy cell
scaled
averages
basket cell (CCK)
10 ms
D
SLM
Ivy cell (M112207s1-18)
SR
SP

Figure S5. Ivy and CCK-expressing basket cells in stratum radiatum have different spike shape and evoke distinct postsynaptic responses. (A) Action potentials (APs) elicited by rectangular depolarising current pulses (90-180 pA) in an Ivy cell (*left*, M102507s7-13) and a CCK-expressing basket cell (*right*, M102407s13-18). Note the pronounced afterhyperpolarisations (AHP) and broad APs in the Ivy cell. (B) *Left*, representative APs evoked in the same Ivy and CCK-expressing basket cell in response to short depolarising current pulses (800 pA, 3 ms) are shown superimposed and aligned on the rising phase. Note that the AP of the Ivy cell is broader than the AP in the CCK-positive basket cell. *Right*, Action potentials (truncated) followed by the AHP in the two cell types. In the Ivy cell (M112207s1-18) the AHP had larger amplitude and shorter duration than in the CCK expressing-basket cell (M102407s13-18). Note that Ivy cells exhibited a single-component, medium-duration AHP, whereas CCK-basket cells displayed a two-component AHP, i.e. a fast initial AHP, followed by a slow component. (C) Unitary inhibitory synaptic currents (uIPSCs) (*upper traces; black traces: average; grey traces: single sweeps*) evoked in two different CA1 pyramidal cells by action currents elicited in an Ivy cell (M112207s22-30) (*middle left trace*) or a CCK-positive basket cell (M111307s4-10) (*middle right trace*). Bottom, the average uIPSCs elicited by the Ivy cell (*black*) and by the CCK expressing-basket cell (*grey trace*) are shown superimposed after scaling. Note that in these recordings, the uIPSC mediated by the Ivy cell was considerably smaller and slower than the one evoked by the CCK positive-basket cell. (D) Reconstruction of the soma, dendrites (red) and axonal processes (yellow) of the recorded Ivy cell (M112207s22-30) from two 70 μm thick sections. SR, stratum radiatum; SP, stratum pyramidale; SO, stratum oriens. Scale bar 100 μm.

Table S1. Proportions of PV and/or NPY and/or nNOS expressing cells determined by the disector method in confocal microscopy

markers	**number of cells**[1]						**cell densities**[2] **(10^3/mm^3)**			
	SO	**SP**	**SR**	**SLM**	**total**	**SO**	**SP**	**SR**	**SLM**	**total**
PV+/NPY+/nNOS-	28	110	3	0	141	0.32 ± 0.10	2.28 ± 0.25	0.01 ± 0.01	0	0.34 ± 0.05
PV-/**NPY+/nNOS+**	42	182	112	14	350	0.48 ± 0.22	3.80 ± 0.54	0.58 ± 0.18	0.16 ± 0.01	0.84 ± 0.07
PV+/NPY-/nNOS-	96	145	5	0	246	1.10 ± 0.17	3.02 ± 0.22	0.02 ± 0.03	0	0.59 ± 0.02
PV-/**NPY+**/nNOS-	51	44	11	20	126	0.58 ± 0.19	0.91 ± 0.29	0.05 ± 0.04	0.24 ± 0.09	0.30 ± 0.10
PV-/NPY-/**nNOS+**	7	20	45	18	90	0.08 ± 0.02	0.42 ± 0.23	0.23 ± 0.03	0.21 ± 0.08	0.22 ± 0.04
PV+/NPY-/**nNOS+**	0	0	0	0	0	0	0	0	0	0
PV+/nNOS+/NPY+	0	0	0	0	0	0	0	0	0	0
total	224	501	176	52	953					

[1] Values represent the numbers of randomly sampled cells according to the optical disector principle (3 animals, 3 sections from each).

[2] Values represent the means ± SD of numerical densities of three animals.

SO, stratum oriens; SP, stratum pyramidale; SR, stratum radiatum; SLM, stratum lacunosum-moleculare

Table S2. Proportions of nNOS and NPY co-expressing cells immunopositive for PV, $GABA_AR$-α1 (countings in all layers); α-actinin-2, calretinin (CR), calbindin (CB) or somatostatin (SM) (countings in stratum pyramidale only) determined by quadruple or triple epi-immunofluorescence-microscopy. Mean ± SD from 3 animals, 1 section from each. Antibodies to NPY were raised in rabbit (CR table, SM table) or sheep ($GABA_A$-α1 table, CB table, α-actinin-2 table) and those to nNOS in mouse ($GABA_A$-α1 table, CR table, CB table) or sheep (SM table) or rabbit (α-actinin-2 table).

	percentages of PV and/or nNOS and/or NPY and/or $GABA_A$-α1 immunopositive cells				
Molecular markers	**SO**	**SP**	**SR**	**SLM**	**total**
PV+/nNOS-/NPY-/ $GABA_AR$-α1-	0%	1.4±2.4%	0%	0%	1.0±1.7%
PV-/**nNOS+**/NPY-/ $GABA_AR$ -α1-	0%	2.5±0.4%	0%	0%	1.8±0.3%
PV-/nNOS-/NPY-/ $GABA_AR$ **-α1+**	8.3±14.4%	1.9±1.3%	7.7±4.9%	32.4±29.3%	4.5±2.6%
PV-/nNOS-/**NPY+**/ $GABA_AR$ -α1-	0%	0%	0%	0%	0%
PV+/nNOS-/NPY-/ $GABA_AR$ **-α1+**	8.3±14.4%	21.5±5.6%	0%	0%	16.4±3.9%
PV+/**nNOS+**/NPY-/ $GABA_AR$ -α1-	0%	0%	0%	0%	0%
PV+/nNOS-/**NPY+**/ $GABA_AR$ -α1-	4.2±7.2%	0%	0%	0%	0.3±0.4%
PV-/**nNOS+**/NPY-/ $GABA_AR$ **-α1+**	3.3±5.8%	5.0±6.6%	1.9±3.2%	38.9±24.1%	6.4±4.4%
PV-/nNOS-/**NPY+**/ $GABA_AR$ **-α1+**	0%	3.8±0.7%	0%	4.2±7.2%	3.1±0.1%
PV-/**nNOS+/NPY+**/ $GABA_AR$ -α1-	0%	0%	0%	0%	0%
PV+/**nNOS+**/NPY-/ $GABA_AR$ **-α1+**	0%	0%	0%	0%	0%
PV+/nNOS-/**NPY+**/ $GABA_AR$ **-α1+**	0%	13.7±7.7%	5.9±5.6%	0%	11.0±6.2%
PV+/**nNOS+/NPY+**/ $GABA_AR$ -α1-	0%	0.3±0.5%	0%	0%	0.2±0.4%
PV-/**nNOS+/NPY+/** $GABA_AR$ **-α1+**	75.8±22.4%	49.4±2.9%	84.5±9.7%	24.5±4.3%	54.9±1.7%
PV+/nNOS+/NPY+/ $GABA_AR$ **-α1+**	0%	0.6±0.5%	0%	0%	0.5±0.4%
total number of cells	22	288	56	20	386

Molecular markers	**percentage**
nNOS-/NPY-/α**-actinin-2+**	3.3±2.9%
nNOS- /**NPY+**/α-actinin-2-	9.2±2.3%
nNOS+/NPY-/α-actinin-2-	13.0±8.1%
nNOS-/**NPY+/α-actinin-2+**	1.1±0.9%
nNOS+/NPY-/α**-actinin-2+**	0.5±0.9%
nNOS+/**NPY+**/α-actinin-2-	18.5±7.1%
nNOS+/NPY+/α-actinin-2+	54.3±6.8%
total number of cells	184

Molecular markers	**percentage**
nNOS-/NPY-/**CB+**	2.5±2.4%
nNOS**-/NPY+**/CB-	16.2±6.0%
nNOS+/NPY-/CB-	7.2±4.2%
nNOS-/**NPY+/CB+**	1.0±1.8%
nNOS+/NPY-/**CB+**	0%
nNOS+/NPY+/CB-	72.6±3.1%
nNOS+/NPY+/CB+	0.5±0.9%
total number of cells	202

Molecular markers	**percentage**
nNOS-/NPY-/**CR+**	8.3±4.3%
nNOS-/**NPY+**/CR-	5.7±3.0%
nNOS+/NPY-/CR-	4.1±2.4%
nNOS-/**NPY+/CR+**	0%
nNOS+/NPY-/**CR+**	2.0±2.2%
nNOS+/NPY+/CR-	77.2±6.4%
nNOS+/NPY+/CR+	2.6±2.3%
total number of cells	154

Molecular markers	**percentage**
nNOS-/NPY-/**SM+**	19.5±4.3%
nNOS-/**NPY+**/SM-	3.7±5.1%
nNOS+/NPY-/SM-	6.0±2.7%
nNOS-/**NPY+/SM+**	10.5±4.9%
nNOS+/NPY-/**SM+**	2.6±0.5%
nNOS+/NPY+/SM-	57.3±5.3%
nNOS+/NPY+/SM+	0.4±0.7%
total number of cells	240

Table S3. Discharge frequencies and preferred firing phase of Ivy cells during theta and gamma oscillations

cell	discharge rate (Hz)			mean phase (°) ± angular deviation		duration (s) or number (*n*) of oscillatory episodes			
	theta	ripples	nt/nr	theta	gamma	theta (s)	gamma (s)	ripples (*n*)	nt/nr (s)
P2a	0.1	0.3	1.8	15 ± 71	9 ± 67	234	865	36	575
T98e	0.6	0.4	1.9	55 ± 58	20 ± 69	240	203	110	142
T134a	0.3	2.4		0 ± 54	52 ± 72	1092	1124	24	
T140b	1.8	0	1.4	53 ± 70	318 ± 64	854	319	30	60

nt/nr, non-theta/non-ripple periods; 0° marks trough of oscillation cycles.

Table S4. List of primary antibodies

antibody	species	dilution	source	specificity reference
α-actinin-2	mouse	1:1000	Sigma, code A7811	Fridlianskaia et al., 1989
	rabbit	1:1000	Dr. A. Beggs, Children's Hospital, Boston, MA, USA, code 4A3	Chan et al., 1998
Calbindin	rabbit	1:5000	Swant, code CB-38	Raised to rat recombinant calbindin. Labeling pattern as published with other antibodies.
	mouse	1:400	Swant, code 300	Celio et al., 1990
CCK	rabbit	1:500	Pro-CCK; Dr. A. Varro, Liverpool University, code L424	Morino et al., 1994
	mouse	1:10000	Dr. G. Ohning, CURE, UCLA, USA, code 9303	Ohning et al., 1996
Calretinin	goat	1:1000	Swant, code CG1	Raised to human recombinant CR. Labeling pattern as published with other antibodies.
$GABA_AR$ α1 subunit	rabbit	0.4µg/ml	Dr. W. Sieghart, Brain Res. Inst., Vienna, Austria	Zezula et al., 1991; Baude et al., 2006, KO test.
GAD	sheep	1:500	Dr. E. Mugnaini, Northwestern Univ., Chicago, USA, code GAD1440-4	Oertel et al., 1980
Kv3.1b	rabbit	0.6µg/ml	Alomone Labs. code APC-014	Raised to residues 567-585 of rat sequence. Western blot, Gelband et al., 1999
M2 receptor	rat	1.4µg/ml	Chemicon, code MAB367	Levey et al., 1995
mGluR1α	guinea pig	0.5µg/ml	Dr. M. Watanabe, Hokkaido University, Japan	Nakamura et al., 2004
mGluR8a	guinea pig	1.1µg/ml	Dr. R. Shigemoto, Natl. Institute Physiol., Okazaki, Japan	Shigemoto et al., 1996
µ opioid receptor	guinea pig	1:1000	Chemicon, code AB1774	Raised to residues 384-398 of rat receptor. Labeling pattern as published with other antibodies.
nNOS	rabbit	1:1000	Chemicon, code AB5380	Raised to recombinant human nNOS. Labeling pattern as published with other antibodies.
	mouse	1:1000	Sigma, code N2280	Raised to recombinant rat nNOS residues 1-181. Labeling pattern as published with other antibodies.
	sheep	1:500	Chemicon, code AB1529	Raised to residues 1409-1429 of rat NOS. Labeling pattern as published with other antibodies.
NPY	rabbit	1:5000	DiaSorin, code 22940	Labeling pattern as published with other antibodies. Absorption tested by manufacturer to 6 other peptides.
	sheep	1:1000	Chemicon, code AB1583	Blessing et al., 1986
PPTA	guinea pig	0.85µg/ml	Dr. T. Kaneko, Kyoto University, Japan	Kaneko et al., 1998
PPTB	guinea pig	0.8µg/ml	Dr. T. Kaneko, Kyoto University, Japan	Kaneko et al., 1998.
Parvalbumin	guinea pig	1:1000	Dr. K.G. Baimbridge, code GP404	Raised to purified rat muscle parvalbumin. Labeling pattern

				as published with other antibodies, and K.G.B. personal communication.
Somatostatin	mouse	1:500	Dr. A. Buchan, Univ. Br. Columbia, Canada, code Soma8	Vincent et al., 1985.
VIP	rabbit	1:2000	Euro-Diagnostica, UK, Code B34-1	Raised to porcin VIP. Labeling pattern as published with other antibodies
	mouse	1:5000	Biogenesis, Code 9535-0504	Dey et al., 1988.

REFERENCES

Baude A, Bleasdale C, Dalezios Y, Somogyi P, Klausberger T (2006) Immunoreactivity for the GABAA Receptor α1 Subunit, Somatostatin and Connexin36 Distinguishes Axoaxonic, Basket, and Bistratified Interneurons of the Rat Hippocampus. Cereb Cortex.

Blessing WW, Howe PR, Joh TH, Oliver JR, Willoughby JO (1986) Distribution of tyrosine hydroxylase and neuropeptide Y-like immunoreactive neurons in rabbit medulla oblongata, with attention to colocalization studies, presumptive adrenaline-synthesizing perikarya, and vagal preganglionic cells. J Comp Neurol 248:285-300.

Celio MR, Baier W, Scharer L, Gregersen HJ, de Viragh PA, Norman AW (1990) Monoclonal antibodies directed against the calcium binding protein Calbindin D-28k. Cell Calcium 11:599-602.

Chan Y, Tong HQ, Beggs AH, Kunkel LM (1998) Human skeletal muscle-specific alpha-actinin-2 and -3 isoforms form homodimers and heterodimers in vitro and in vivo. Biochem Biophys Res Commun 248:134-139.

Dey RD, Hoffpauir J, Said SI (1988) Co-localization of vasoactive intestinal peptide- and substance P-containing nerves in cat bronchi. Neuroscience 24:275-281.

Fridlianskaia, II, Goncharova EI, Borisov AB, Krylova TA, Pinaev GP (1989) [Monoclonal antibodies to the muscle isoform of alpha-actinin--a marker for the study of the differentiation of skeletal and cardiac muscles]. Tsitologiia 31:1234-1237.

Gelband CH, Warth JD, Mason HS, Zhu M, Moore JM, Kenyon JL, Horowitz B, Sumners C (1999) Angiotensin II type 1 receptor-mediated inhibition of K+ channel subunit kv2.2 in brain stem and hypothalamic neurons. Circ Res 84:352-359.

Kaneko T, Murashima M, Lee T, Mizuno N (1998) Characterization of neocortical non-pyramidal neurons expressing preprotachykinins A and B: a double immunofluorescence study in the rat. Neuroscience 86:765-781.

Levey MS, Brumwell CL, Dryer SE, Jacob MH (1995) Innervation and target tissue interactions differentially regulate acetylcholine receptor subunit mRNA levels in developing neurons in situ. Neuron 14:153-162.

Nakamura M, Sato K, Fukaya M, Araishi K, Aiba A, Kano M, Watanabe M (2004) Signaling complex formation of phospholipase Cbeta4 with metabotropic glutamate receptor type 1alpha and 1,4,5-trisphosphate receptor at the perisynapse and endoplasmic reticulum in the mouse brain. Eur J Neurosci 20:2929-2944.

Oertel WH, Schmechel DE, Daly JW, Tappaz ML, Kopin IJ (1980) Localization of glutamate decarboxylase on line-immunoelectrophoresis and two-dimensional electrophoresis by use of the radioactive suicide substrate [2-3H]-gamma-acetylenic GABA. Life Sci 27:2133-2141.

Ohning GV, Wong HC, Lloyd KC, Walsh JH (1996) Gastrin mediates the gastric mucosal proliferative response to feeding. Am J Physiol 271:G470-476.

Shigemoto R, Kulik A, Roberts JD, Ohishi H, Nusser Z, Kaneko T, Somogyi P (1996) Target-cell-specific concentration of a metabotropic glutamate receptor in the presynaptic active zone. Nature 381:523-525.

Vincent SR, McIntosh CH, Buchan AM, Brown JC (1985) Central somatostatin systems revealed with monoclonal antibodies. J Comp Neurol 238:169-186.

Zezula J, Sieghart W (1991) Isolation of type I and type II GABAA-benzodiazepine receptors by immunoaffinity chromatography. FEBS Lett 284:15-18.

Table S5. Comparison of action potentials, membrane properties, molecular expression of Ivy and CCK-basket cells and the properties of their synaptic connections with CA1 pyramidal cells recorded intracellularly in stratum radiatum *in vitro*

	Action potential			intrinsic membrane properties			molecular markers			
interneuron type	**half width (ms)**	**AHP amplitude (mV)**	**AHP half width (ms)**	**Input resistance (MΩ)**	**time constant (ms)**	**resting potential (mV)**	**nNOS**	**NPY**	**CCK**	**CB1R**
Ivy										
m101907s7-s8	1.1	20.2	38.8	399	29.2	-69.7	+	nt	nt	-
m102507s10-s11	1.3	19	42.6	468	15.1	-67.5	+	+	-	-
m102507s2-s4	0.9	14.6	27	443	23.2	-61	nt	nt	nt	-
m112207s1-s18	1	20.6	32.8	357	27.2	-63.7	+	+	nt	-
m112207s22-s32	0.9	22.3	26.6	287	19.7	-58.2	+	+	nt	-
mean±SD	1.0±0.2*	19.3±2.9	33.6±7.1*	390.8±71.9	22.9±5.7	-64.0±4.7				
CCK-basket										
m101907s3-s4	0.7	12.6	51.7	327	47.6	-64.9	-	nt	+	+
m102407s1-s12	0.8	6.7	55.6	315	28.6	-66	-	-	+	+
m102407s15-s16	0.8	17.1	103.8	699	51.5	-60.8	-	-	+	+
m111307s4-s10	0.6	14.7	43.6	489	24.1	-61.1	nt	nt	+	+
m111307s11-s34	0.8	17.2	42.1	465	51.9	-60.8	nt	nt	+	+
mean±SD	0.7±0.1	13.7±4.3	59.4±25.5	459.0±155.5	40.7±13.3	-62.7±2.5				

presynaptic interneuron	**evoked IPSCs in CA1 pyramidal cells**					
Ivy	**amplitude (pA)**	**10-90% rise time (ms)**	**half width (ms)**	**decay time (ms)**	**failure rate (%)**	**postsynaptic holding potential (mV)**
m112207s22-s32	9.9	3	17.8	13.6	48	-50
m112207s1-s18	6.1	2.6	15.8	18.5	54	-50
CCK-basket						
m111307s4-s10	31.9	1.2	8.3	7.4	58	-50
m111307s11-s34	15.4	2.8	10.4	8.9	50	-50

AHP, afterhyperpolarization; * indicates statistcal significance at $P < 0.05$; nt, not tested.